Available online at www.sciencedirect.com
ScienceDirect
Remote Sensing of Environment 112 (2008) 2677–2685
Remote Sensing of Environment
www.elsevier.com/locate/rse

Remote sensing of ocean color: Assessment of the water-leaving radiance bidirectional effects on the atmospheric diffuse transmittance for SeaWiFS and MODIS intercomparisons

Howard R. Gordon [a,*], Bryan A. Franz [b]

[a] Department of Physics, University of Miami, Coral Gables, FL 33124, United States
[b] SAIC, Ocean Biology Processing Group, NASA/GSFC, Greenbelt, MD 20771, United States

Received 18 October 2007; received in revised form 14 December 2007; accepted 22 December 2007

Abstract

The portion of the radiance exiting the ocean and transmitted to the top of the atmosphere (TOA) in a particular direction depends on the angular distribution of the exiting radiance, not just the radiance exiting in the direction of interest. The diffuse transmittance t relates the water component of the TOA radiance to that exiting the water in the *same* direction. As such t is a property of the ocean–atmosphere system and not just the atmosphere. Its computation requires not only the properties of the atmosphere but the angular distribution of the exiting radiance as well. The latter is not known until a determination of the water properties can be made (which is the point of measuring the radiance in the first place). Because of this, it has been customary to assume an angular distribution (uniform upward radiance *beneath* the water surface) in the computation of t, which is referred to as t^*. However, it is known that replacing t with t^* can result in an error of several percent in the retrieved water-leaving radiance. Since the error depends on sun-viewing direction, this error could be particularly important when water-leaving radiance from two or more sensors in different orbits are compared. Even given an estimate of the angular distribution of the water-leaving radiance, computation of t using full radiative transfer theory in an image processing environment is not practical. Thus, we developed a first-order correction to t for bidirectional effects in the water-leaving radiance that captures much of the variability of t with viewing direction. The correction computed across a SeaWiFS scan line shows that a t^*-induced error of as much as 5–6% could occur near the edges of the scan; however, limiting the scan to polar viewing angles (θ) $<60°$ reduces the error to ~1%. Direct application to SeaWIFS and MODIS (AQUA) suggests that the bidirectionally-induced error in the diffuse transmittance will result in an error less than about 1% in the comparison of their normalized water-leaving radiances, as long as θ is less than about 60°. We conclude that, given this constraint, the normalized water-leaving retrievals from these two sensors at a given location can be merged without regard for the bidirectionally-induced error in the diffuse transmittance, as the resulting uncertainty is well below that from other sources. It is important to note that this result is likely to apply to any other polar-orbiting sensor with equatorial crossing times (similar to SeaWiFS and MODIS) between 1030 and 1330 h (local time).

Keywords: Ocean Color; Diffuse Transmittance; Bidirectionality; SeaWIFS; MODIS

1. Introduction

The concentration of marine phytoplankton in the world oceans is now being monitored using earth-orbiting sensors, i.e., the Coastal Zone Color Scanner (CZCS) (Gordon et al., 1980; Hovis et al., 1980), the sea-viewing wide-field-of-view sensor (SeaWiFS) (Hooker et al., 1992), the moderate resolution imaging spectroradiometer (MODIS) (Salomonson et al., 1989), etc. Such monitoring is effected by quantitatively measuring absorption of solar radiation by the photosynthetic pigment chlorophyll *a* within the phytoplankton. This absorption is manifest in a decrease in the radiance backscattered from the water and transmitted to the top of the atmosphere in the blue region of the spectrum. Although this monitoring has become more-or-less routine, there are still issues that are ignored even in first-order.

Briefly, the radiance exiting the top of the atmosphere (TOA) in the direction $\hat{\xi}$ in a spectral band centered at λ_i, $L_t(\hat{\xi},\lambda_i)$, can be written

$$L_t(\hat{\xi},\lambda_i) = L_{\text{Other}}(\hat{\xi},\lambda_i) + L_w^{\text{TOA}}(\hat{\xi},\lambda_i) \quad (1)$$

* Corresponding author.
E-mail address: gordon@physics.miami.edu (H.R. Gordon).

0034-4257/$ - see front matter © 2008 Elsevier Inc. All rights reserved.
doi:10.1016/j.rse.2007.12.010

where $L_{\text{Other}}(\hat{\xi},\lambda_i)$ represents the contribution to the radiance from all sources except the water-leaving radiance (radiance backscattered *out* of the water) and transmitted to the TOA, $L_w^{TOA}(\hat{\xi},\lambda_i)$. Sources of $L_{\text{Other}}(\hat{\xi},\lambda_i)$ include scattering of solar radiation in the atmosphere, reflection of scattered and unscattered radiation from the direct solar beam by the air–sea interface (Fresnel reflection), and scattering from oceanic whitecaps. The atmospheric correction algorithm of Gordon and Wang (1994) estimates $L_{\text{Other}}(\hat{\xi},\lambda_i)$ and removes it from the total radiance, obtaining an estimate of the water-leaving radiance that was transmitted to the top of the atmosphere, $L_w^{TOA}(\hat{\xi},\lambda_i)$. However, algorithms for estimating phytoplankton absorption are based on the water-leaving radiance at the water surface, $L_w(\hat{\xi},\lambda_i)$, not at the TOA. This is related to $L_w^{TOA}(\hat{\xi},\lambda_i)$ through the diffuse transmittance of the atmosphere.

In general, radiance exits the water and enters the atmosphere in all upward directions. It is then modified by the atmosphere through absorption and scattering and exits the top of the atmosphere, where it is measured by the sensor. The diffuse transmittance is defined through

$$t(\hat{\xi},\lambda_i) = \frac{L_w^{TOA}(\hat{\xi},\lambda_i)}{L_w(\hat{\xi},\lambda_i)},$$

i.e., the radiance exiting the top of the atmosphere in the direction $\hat{\xi}$ divided by the radiance entering the bottom of the atmosphere propagating in the *same* direction. Here, and henceforth, to avoid symbol clutter we drop the λ_i with the understanding that all nongeometrical quantities depend on wavelength. Note that t need not be less than unity: if a given direction $\hat{\xi}$ happened to be at a deep minimum in $L_w(\hat{\xi})$, then scattering of radiance $L_w(\hat{\xi}')$ by the atmosphere from other directions $\hat{\xi}' \neq \hat{\xi}$ into $\hat{\xi}$ could result in $L_w^{TOA}(\xi)$ being larger than $L_w(\hat{\xi})$. Thus, it is clear that t is not a property of the atmosphere alone; it also depends on the angular distribution of L_w. However, because radiative transfer is a linear process, it does not depend on the absolute magnitude of L_w.

Computing the diffuse transmittance is straightforward in principle: illuminate the bottom of the atmosphere by radiance with the angular distribution characteristic of $L_w(\hat{\xi})$ and compute the radiance exiting the TOA. However, even if the optical properties of the atmosphere and the angular distribution of L_w were precisely known, determination of t requires a full solution of the equation of radiative transfer — a task that is not feasible at this time in an image processing environment. Thus, an approximation for t is used in processing satellite imagery.

Yang and Gordon (1997) formulated a method for computing the diffuse transmittance using the reciprocity principle. This method becomes particularly efficient when the upward radiance just beneath the water surface, $L_u(\hat{\xi})$, is totally diffuse, i.e., is independent of the propagation direction. In addition, as observations suggest that $L_u(\hat{\xi})$ is not a strong function of $\hat{\xi}$, varying by at most a factor of two or three over the relevant range of viewing directions, it is natural to consider the special case where the upwelling radiance just beneath the surface is uniform. The diffuse reflectance in this approximation is referred to as t^*. Since L_w (and certainly its angular distribution) is in fact *a priori* unknown, here-to-fore the assumption of uniform subsurface upward radiance has been used to retrieve $L_w(\hat{\xi})$ from $L_w^{TOA}(\xi)$, i.e., t has been approximated by t^*. Since the Gordon and Wang (1994) algorithm uses a specific set of aerosol models for computation of $L_{\text{Other}}(\hat{\xi})$, it is possible to precompute tables of t^* for each model, and therefore carry out a completely consistent analysis of both terms in Eq. (1) — the only approximation being the use of t^* in place of t.

Using measured $L_u(\hat{\xi})$ distributions, Yang and Gordon (1997) investigated the magnitude of the error that could result from using t^* in place of t and found that it could be as much as ±5−6% or more in the retrieved value of L_w, depending on the sun-viewing geometry and the dependence of $L_u(\hat{\xi})$ on $\hat{\xi}$. The error is generally largest viewing in the principal plane (the plane containing the sun and the zenith) and smallest in the perpendicular plane. This error is over-and-above that caused by the error in estimating $L_{\text{Other}}(\hat{\xi})$. It is also the same order as the uncertainty goal for L_w for most ocean color sensors. For SeaWiFS, which usually views close to the perpendicular plane, the error should be small; however, for MODIS, viewing close to the principal plane is not uncommon, so the error could be significant. More importantly, the error can cause *systematic* differences between water-leaving radiances derived from sensors on satellites with differing orbital characteristics.

Even given the angular distribution of L_w at the sea surface, a model of which is now available for Case 1 (Gordon & Morel, 1983) oceanic waters given an estimate of the concentration of chlorophyll *a* (Morel & Gentili, 1991, 1993, 1996; Morel et al., 1995, 2002), computation of the diffuse reflectance still requires a full solution of the equation of radiative transfer for the particular geometry, and is thus unsuitable for processing satellite imagery. Here we provide first-order approximations of t and t^* suitable for image processing, and show that they can be used to provide an improvement over simply using t^* as a substitute for t. We then apply this approximation to SeaWiFS and MODIS imagery.

2. First-order approximation of the diffuse reflectance

The radiative transfer problem that must be solved in first-order consists of finding the radiance $L_w^{TOA}(\xi)$ exiting the top of the atmosphere measured by a radiometer (aimed toward $-\hat{\xi}$), given radiance $L_w(\hat{\xi}')$ exiting the water entering the bottom of the atmosphere, where $\hat{\xi}'$ is a unit vector pointing in *any* upward direction.

The direction $\hat{\xi}$ will be specified as follows. Consider a Cartesian coordinate system with the z-axis pointed toward the water and the x–y plane parallel to the water surface. Let $\hat{e}_x$, $\hat{e}_y$ and $\hat{e}_z$ be unit vectors in the x, y, and z directions, respectively. Then $\hat{\xi}$ is given by

$$\hat{\xi} = \hat{e}_x \sin\theta\cos\phi + \hat{e}_y \sin\theta\sin\phi + \hat{e}_z\cos\theta,$$

where θ is the angle between the propagation direction and the $+z$-axis, and ϕ is the azimuth angle in the x–y plane. In what follows, we will abandon the use of θ in favor of $u = \cos\theta$. Radiance propagating toward the water surface has positive u, while radiance exiting the water has negative values of u.

If τ is the optical depth of the atmosphere then, in the first-order approximation (single-scattering limit as $\tau \to 0$), the diffuse transmittance is easily shown to be

$$t_{SS}(u,\phi) = \frac{L_w^{TOA}(u,\phi)}{L_w(u,\phi)} = 1 - \frac{\tau}{|u|}\left(1 - \frac{\omega_0}{4\pi}\int_{-1}^{0} du' \int_0^{2\pi} d\phi' P(u' \to u, \phi' \to \phi)\frac{L_w(u',\phi')}{L_w(u,\phi)}\right)$$

where ω_0 is the single-scattering albedo of the atmosphere and $P(u' \to u, \phi' \to \phi)$ is the phase function for scattering from (u', ϕ') to (u, ϕ), normalized to 4π. The scattering phase function and single-scattering albedo product can be written in terms of its molecular (Rayleigh) and aerosol components:

$$\omega_0 \tau P = \omega_r \tau_r P_r + \omega_a \tau_a P_a$$

where the subscripts r and a refer to Rayleigh and aerosol respectively. Anticipating that t_{SS} is close to unity, we use the approximation $\exp(-x) \cong 1 - x$ to obtain

$$t_{SS}(u,\phi) = \exp\left[-\frac{\tau}{|u|}\left(1 - \frac{\omega_0}{4\pi}\int_{-1}^{0} du' \int_0^{2\pi} d\phi' P(u' \to u, \phi' \to \phi)\frac{L_w(u',\phi')}{L_w(u,\phi)}\right)\right].$$

Note, although writing t_{SS} in the exponential form above is not necessary, it will be useful later to demonstrate an often-used approximation for t^* in the absence of aerosols.

If the contribution of radiance $L_w(u', \phi')$ backscattered by the atmosphere in a direction u toward the sea surface and then specularly reflected from the water toward the sensor is included, t_{SS} is modified to

$$t_{SS}(u,\phi) = \exp\left[-\frac{\tau}{|u|}\left(1 - \frac{\omega_0}{4\pi}\int_{-1}^{0} du' \int_0^{2\pi} d\phi' P(u' \to u, \phi' \to \phi)\frac{L_w(u',\phi')}{L_w(u,\phi)}\right)\right] \times \exp\left[-\frac{\tau}{|u|}\left(-\frac{\omega_0}{4\pi}\int_{-1}^{0} du' \int_0^{2\pi} d\phi' R_f(-u) P(u' \to -u, \phi' \to \phi)\frac{L_w(u',\phi')}{L_w(u,\phi)}\right)\right] \quad (2)$$

where $R_f(-u)$ is the Fresnel reflectance of the water surface (radiance propagating in the direction (u, ϕ) reflected into the direction $(-u, \phi)$. We note in passing that in the case of pure Rayleigh scattering ($\omega_0 = 1$), and if the term containing the surface reflectance is ignored, then when $L_w(u', \phi')$ is totally diffuse, i.e., independent of u' and ϕ', the integral is 2π and the diffuse transmittance becomes $\exp[-\tau_r/2|u|]$, the approximation employed by Gordon et al. (1983).

Evaluation of these integrals is most efficiently effected by noting that the water-leaving radiance is a slowly varying function of azimuth and can therefore be represented by a Fourier series in azimuth with a small number of terms. That is

$$L_w(u,\phi) = L_w^{(0)}(u) + 2\sum_{m=1}^{M} L_w^{(m)}(u)\cos m(\phi - \phi_0), \quad (3)$$

where

$$L_w^{(m)}(u) = \frac{1}{2\pi}\int_0^{2\pi} L_w(u,\phi)\cos m(\phi - \phi_0) d\phi,$$

and ϕ_0 is the solar azimuth angle. We expect M to be small, e.g., 3 or 4. In a similar manner the scattering phase function can be expanded in a Fourier series,

$$P(u' \to u, \phi' \to \phi) = p^{(0)}(u' \to u) + 2\sum_{\ell=1}^{\infty} p^{(\ell)}(u' \to u)\cos \ell(\phi' - \phi), \quad (4)$$

where the Fourier coefficients are given by

$$p^{(\ell)}(u' \to u) = \frac{1}{2\pi}\int_0^{2\pi} d\phi' P(u' \to u, \phi' \to \phi)\cos \ell(\phi' - \phi) = \frac{1}{2\pi}\int_0^{2\pi} d\phi\, P(u' \to u, \phi' \to \phi)\cos \ell(\phi' - \phi).$$

Inserting the Fourier series into Eq. (2) and carrying out the integration over ϕ' yields

$$t_{SS}(u,\phi) = \exp\left[-\frac{\tau}{|u|}\left(1 - \frac{\omega_0}{2}\int_{-1}^{0} du' \left\{p^{(0)}(u' \to u) + R_f(-u)p^{(0)}(u' \to -u)\right\}\frac{L_w^{(0)}(u')}{L_w(u,\phi)}\right)\right] \times \exp\left[\frac{\tau}{|u|}\left(\omega_0 \int_{-1}^{0} du' \sum_{m-1}^{M} \left\{p^{(m)}(u' \to u) + R_f(-u)p^{(m)}(u' \to -u)\right\}\frac{L_w^{(m)}(u')}{L_w(u,\phi)}\cos m(\phi - \phi_0)\right)\right]. \quad (5)$$

If desired, the water-leaving radiance $L_w(u', \phi')$ can be written in terms of the upwelling radiance just beneath the surface $L_u(u'_w, \phi')$ according to

$$L_w(u', \phi') = \frac{T_f(u'_w \to u')L_u(u'_w, \phi')}{n_w^2}$$

where T_f is the Fresnel transmittance, n_w is the refractive index of water, and u' and u'_w are related by Snell's law. In the special case where the upwelling radiance just beneath the surface is uniform the diffuse transmittance becomes

$$t_{SS}^*(u,\phi) = \exp\left[-\frac{\tau}{|u|}\left(1 - \frac{\omega_0}{2}\int_{-1}^{0} du' \left\{p^{(0)}(u' \to u) + R_f(-u)p^{(0)}(u' \to -u)\right\}\frac{T_f(u'_w \to u')}{T_f(u_w \to u)}\right)\right]. \quad (6)$$

To gauge the efficacy of this single-scattering development, we make comparisons with the exact computation of Yang and Gordon (1997). They computed

$$\delta(\hat{\xi}) \equiv \frac{t(\hat{\xi}) - t^*(\hat{\xi})}{t^*(\hat{\xi})},$$

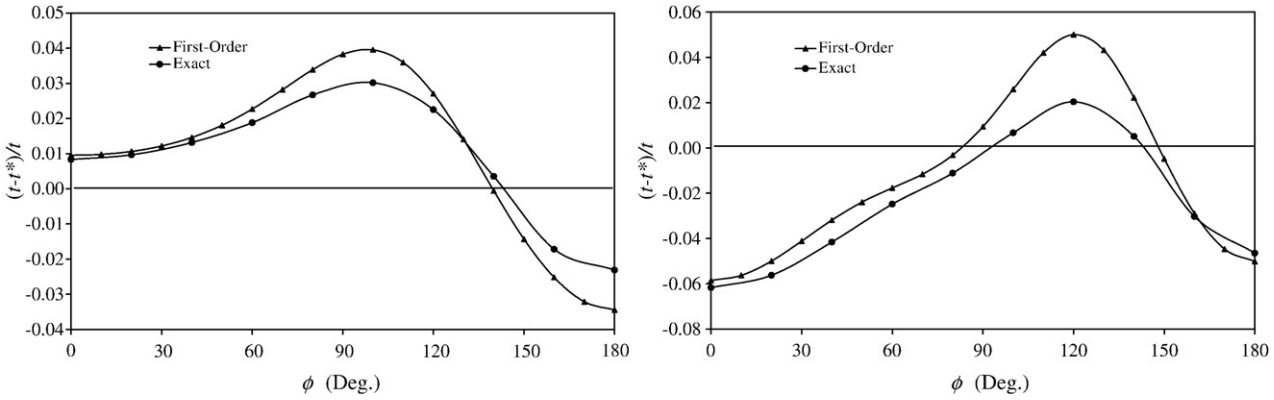

Fig. 1. Comparison of δ computed exactly by Yang and Gordon (1997) ("Exact") with δ_{SS} computed using the single-scattering development ("First-order"). The wavelength is 443 nm, the solar zenith angle is 40° (left panel) and 60° (right panel), the aerosol is modeled as M90 (Gordon & Wang, 1994; Shettle & Fenn, 1979) with τ_a=0.2, and the viewing angle is equal to θ_0.

the error in the retrieved $L_w(\hat{\xi})$ when $t^*(\hat{\xi})$ is used in place of $t(\hat{\xi})$, for several subsurface upwelling radiance distributions $L_u(u'_w, \phi')$. For the comparison, we used $L_u(u'_w, \phi')$ generated by "Petzold's" phase function (See Yang and Gordon (1997) for details, but note that ϕ in the present paper is $\pi-\phi$ in Yang and Gordon). The weak dependence of $L_u(u'_w, \phi')$ on the relative azimuth suggests that M (the maximum Fourier order) in Eq. (3) need not be large. In fact, for all the first-order computations we present here M=3 or 4. The maximum value of ✓ required for the decomposition of the azimuthal dependence of the aerosol phase function is likewise M. Fig. 1 compares the computation of

$$\delta_{SS}(\hat{\xi}) \equiv \frac{t_{SS}(\hat{\xi}) - t^*_{SS}(\hat{\xi})}{t^*_{SS}(\hat{\xi})},$$

with the Yang and Gordon (1997) exact computation δ as a function of the viewing relative (to the sun) azimuth angle ϕ for θ_0=40°and 60°, at 443 nm with τ_a=0.2. The aerosol properties are those of M90 (the maritime model of Shettle and Fenn (1979) at 90% relative humidity). For this computation, we used M=4 for which the average error in $L_w(u, \phi)$ for $\theta=\theta_0$=60° reconstructed from $L_w^{(m)}(u)$ using Eq. (3) was ~1%. Increasing M above 4 had virtually no effect on the resulting $\delta_{SS}(\hat{\xi})$. The single-scattering computation is clearly in qualitative agreement with the exact result; however, the error in $\delta_{SS}(\hat{\xi})$can be as much as a factor of 2 with respect to $\delta(\hat{\xi})$. We carried out similar computations for 555 nm and found even closer agreement between $\delta_{SS}(\hat{\xi})$ and $\delta(\hat{\xi})$ (not shown).

3. Retrieval of L_w using the first-order diffuse transmittance

Although there can be significant error in $\delta_{SS}(\hat{\xi})$, it can still be used to provide a first-order correction for directional effects on the retrieval of $L_w(\hat{\xi})$. If $L_w^{TOA}(\hat{\xi})$ is considered to be exact, then the retrieval

$$L_w(\hat{\xi}) = \frac{L_w^{TOA}(\hat{\xi})}{t^*(\hat{\xi})(1+\delta(\hat{\xi}))}$$

will be exact in contrast to the traditional retrieval:

$$L^*_w(\hat{\xi}) = \frac{L_w^{TOA}(\hat{\xi})}{t^*(\hat{\xi})}.$$

One can improve on the traditional retrieval by replacing $L^*_w(\hat{\xi})$ by

$$\frac{L_w^{TOA}(\hat{\xi})}{t^*(\hat{\xi})(1+\delta_{SS}(\hat{\xi}))}.$$

Because $\delta_{SS}(\hat{\xi})$ captures much of the variation with direction of its exact counterpart, the retrieved $L_w(\hat{\xi})$ will be freer of directional bias than the traditional retrieval, making intercomparison of sensors in different orbits more meaningful.

Morel, Gentili and coworkers (Morel & Gentili, 1991, 1993, 1996; Morel et al., 1995, 2002) have presented a model of the subsurface upwelling radiance distribution in which, apart from constant factors, the upwelling radiance $L_u(\hat{\xi})$ is given by

$$L_u(\hat{\xi}) = \frac{f}{Q}\frac{b_b}{a}$$

where a and b_b are, respectively, the absorption and backscattering coefficients of the water body. All of the angular effects are manifest in f/Q. Fig. 2 provides this quantity (as modeled by Morel et al. (2002) for oceanic water) for low and high chlorophyll concentrations for a solar zenith angle of 60°. Note the qualitative difference in the behavior of f/Q for the two cases: low chlorophyll shows a maximum in backscattered directions (ϕ=180°); high chlorophyll shows a maximum in forward scattered directions (ϕ=0°). Reconstruction of f/Q from its Fourier transform was accurate to within 0.25% for $\theta=\theta_0$=60° with M=3. In addition, the Fourier coefficients (normalized to those at m=0) were significantly smaller than for the Petzold L_w used in the preparation of Fig. 1. This smoothness of the Morel and Gentili L_w compared to the Petzold L_w allowed the use of M=3 in the computation of $\delta_{SS}(\hat{\xi})$ rather than M=4.

Fig. 3 provides examples of $\delta_{SS}(\hat{\xi})$ computed using Eq. (5) (λ=443 nm, M90 aerosol, τ_a=0.2) with $L_u(\hat{\xi})$ (actually, f/Q) given by the models in Fig. 2. The figures show that the t^*-induced

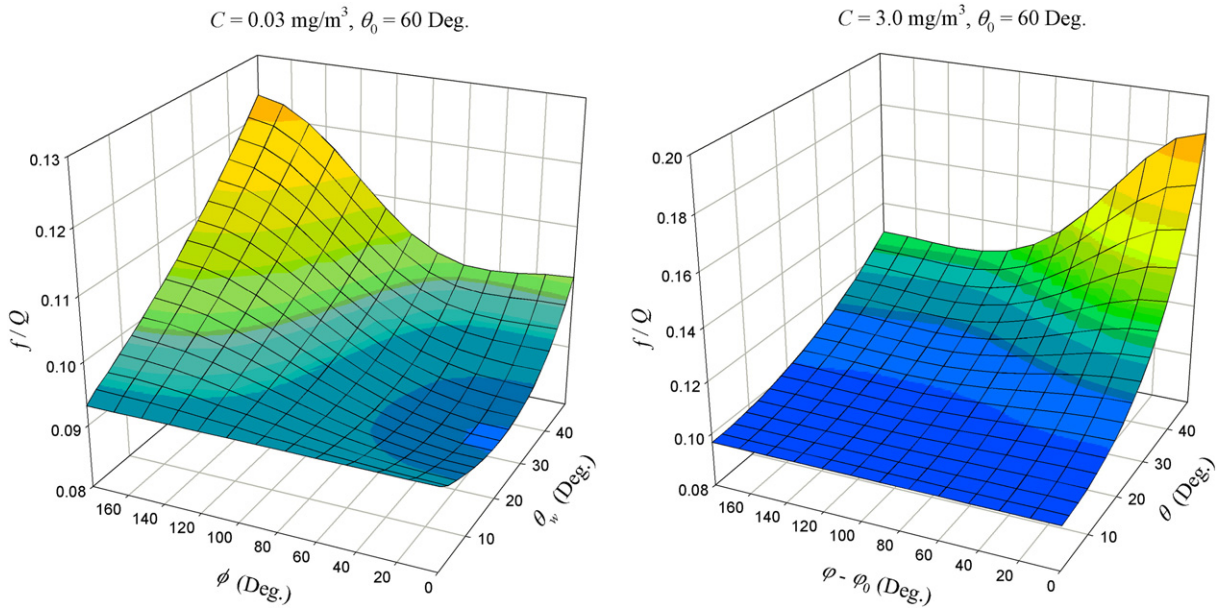

Fig. 2. Variation of f/Q at 443 nm with viewing direction for low (left panel) and high (right panel) chlorophyll concentrations. The solar zenith angle is 60°. The upward-propagating L_u makes an angle θ_w with the zenith, and an azimuth angle of ϕ relative to the solar azimuth. Note that the vertical scale in left panel is expanded compared to that in the right panel.

error grows significantly with increasing θ. Of the U.S. ocean color sensors launched in 1997 or later, SeaWiFS is in an orbit crossing the Equator near local noon, while the MODIS instruments are in orbits that cross approximately ±1.5 h of local noon. Fig. 4 is a polar plot comparing the range of viewing geometries of MODIS (left) and SeaWiFS (right). Each dot represents a different viewing azimuth (relative to the sun) and zenith angles in an orbit. The zenith angle ranges from 0° at the center of the figure radially to the maximum viewing zenith at the edge of the scan. The relative azimuth ranges from 0° ("looking toward the sun") to 180° ("looking away from sun"). These were taken from 3 orbits (Northern Hemisphere summer, fall, and winter) restricted between 70°N and 70°S. The density of points is proportional to the density of viewing directions with a given zenith and relative azimuth. The SeaWiFS viewing geometry is seen to be much more restricted in zenith and azimuth than MODIS. In fact MODIS can have nearly *any* relative azimuth. Note, as SeaWiFS has the capability of tilting the scan plane to avoid sun glint, its minimum θ is about 23°, resulting in an absence of views near nadir ($\theta=0°$). Fig. 3 suggests that intercomparing the retrieval of $L_w(\hat{\xi})$ using t^* for these two instruments might include systematic biases, that could be as high a 5%, especially at low and high chlorophyll levels. These biases can be reduced using $\delta_{SS}(\hat{\xi})$.

Although it represents an enormous simplification over the exact computations, deriving t using Eq. (5) is still too slow to be used in an image processing environment. Thus, two modifications have been made to increase the computational speed of the single-scattering computation. The first is to compute $t^*_{SS}(u,\phi)$ for both the molecular and aerosol components

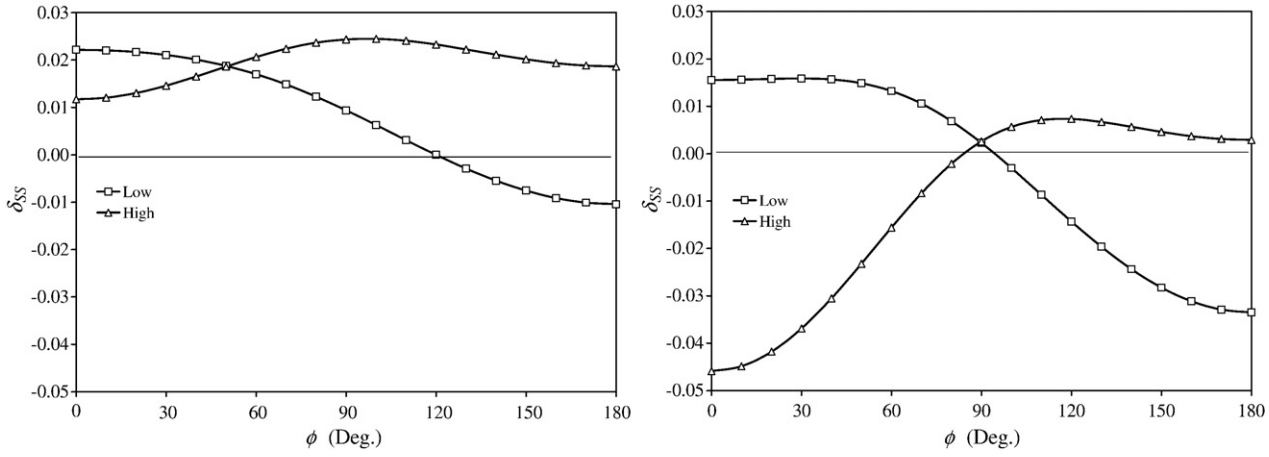

Fig. 3. The correction, δ_{SS}, for the high and low chlorophyll radiance distributions shown in Fig. 2 for the geometry with $\theta=40°$ and $\theta_0=60°$ (left panel) and $\theta=\theta_0=60°$ (right panel), as a function of the relative azimuth. The wavelength is 443 nm and the aerosol model is M90 with $\tau_a=0.2$.

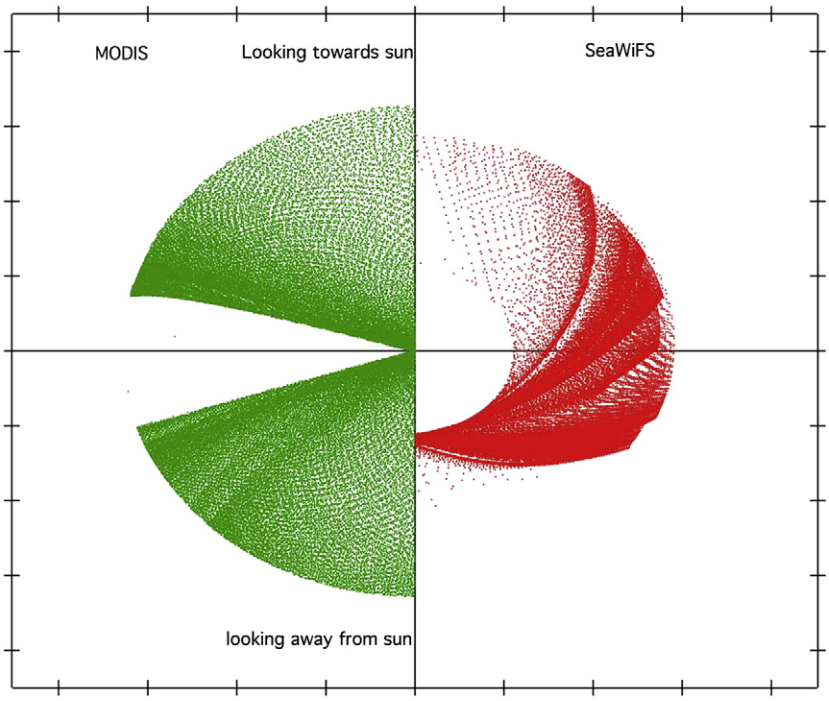

Fig. 4. Polar plot of the viewing geometry for MODIS and SeaWiFS. The center is viewing toward the nadir. The viewing angle θ is linear in the radial direction up to the maximum for a given sensor. The tick marks along the horizontal and vertical axes are every 20° in θ. The relative azimuth ϕ is the polar angle on this plot, with ϕ=0° at the top and 180° at the bottom. The full scan is shown for MODIS, while only the narrower GAC (Global Area Coverage) scan is shown for SeaWiFS.

once-and-for-all and store the results in look up tables (LUTs). The second is to notice that $p^{(0)}(u'\rightarrow u)$ and $p^{(\curvearrowleft)}(u'\rightarrow u)$ vary much more rapidly with u' than do $L_w^{(0)}(u)$and $L_w^{(m)}(u)$. Because of this, we can break the integration over u' into a small number of intervals treating $L_w^{(0)}(u)$ and $L_w^{(m)}(u)$ (or actually $L_w^{(0)}(u'_w)$ and $L_w^{(m)}(u'_w)$ as constants in each interval. We use ten intervals equally spaced in θ. For each interval the subsurface upwelling radiance L_u (actually, f/Q) is averaged to form $\langle L_u^{(m)}\rangle$, the mean $L_u^{(m)}(u')$ for $u'_i \le u' \le u'_{i+1}$. Then the products of the phase function and the Fresnel transmittances are integrated to form

$$P_i^{(m)} = \int_{u'_i}^{u'_{i+1}} du' \left[p^{(m)}(u'\rightarrow u) + R_f(-u)p^{(m)}(u'\rightarrow -u)\right] T_f(u'_w \rightarrow u').$$

Then,

$$t_{SS}(u,\phi) = \exp\Big[-\frac{\tau}{|u|}\Big(1-\frac{\omega_0}{2}\frac{1}{T_f(u_w\rightarrow u)L_u(u,\phi)} \times \sum_{i=1}^{10}\sum_{m=0}^{M}\left(2-\delta_{0,m}\right)P_i^{(m)}\langle L_u^{(m)}\rangle_i \cos m(\phi-\phi_0)\Big)\Big],$$

where $\delta_{0,m}$ is 1 if m=0, and zero otherwise. This procedure effectively decouples the chlorophyll concentration, which determines L_u, from the integrations. The efficacy of this procedure is provided in Fig. 5, which compares it to the high resolution (and computationally slow) evaluations of t_{SS} and t^*_{SS} using Eqs. (5) and (6), respectively. The error in evaluating the integrals in this manner is clearly insignificant compared to the inherent error in the procedure itself (Fig. 1).

4. Application to SeaWiFS and MODIS data

Although Eq. (3) and (4) suggest that, because the sun-viewing geometries of SeaWiFS and MODIS are so different, the error incurred using t^* in place of t could be significant, the only way to determine whether or not the correction is actually important is to apply it to the satellite data. The equations developed here were applied to the computation of δ_{SS} as follows.

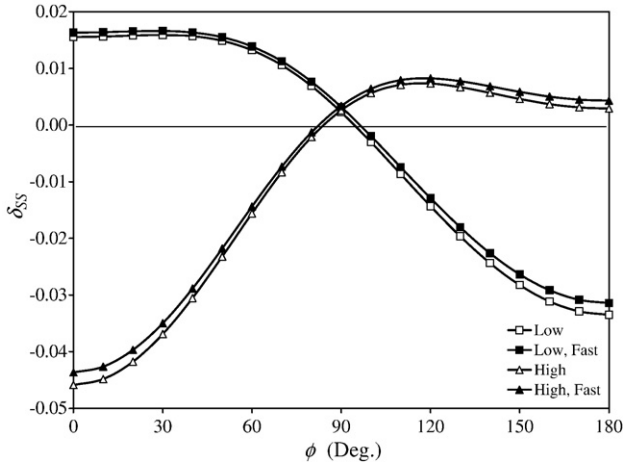

Fig. 5. The correction, δ_{SS}, for the high and low chlorophyll radiance distributions shown in Fig. 2 for the geometry with $\theta=\theta_0$=60°, as a function of the relative azimuth. The wavelength is 443 nm and the aerosol model is M90 with τ_a=0.2. "Low" and "High" refer to the single-scattering computations carried out as in Fig. 3, while "Low, Fast" and "High, Fast" refer to computations carried out with the approximations described in the text to improve the speed of the computation of δ_{SS}.

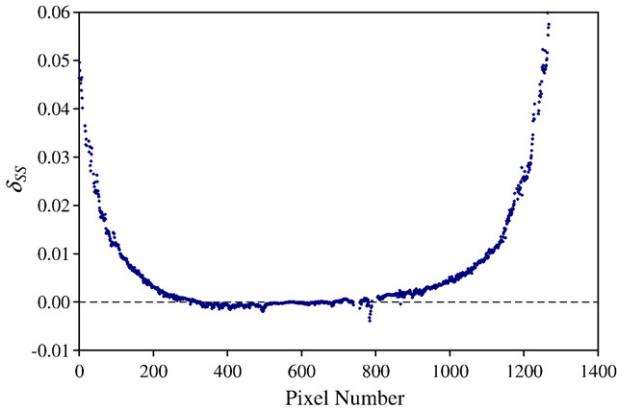

Fig. 6. The factor δ_{SS} as a function of pixel number across a SeaWiFS scan line. This scan line is over the open ocean near Hawaii. The chlorophyll concentration is ~0.1 to 0.2 mg/m^3. The sun angle is 20.6° near the scan center. Pixel number 0 is at the eastern edge of the scan and number 1284 is at the western edge. At the edges of the scan $\theta = 74.16°$. The pixel numbers for $\theta = 60°$ are 106 and 1164.

First, the Gordon and Wang algorithm was applied to remove L_{Other} from L_t to provide L_w^{TOA}. During this procedure, the atmospheric correction algorithm yields two aerosol models (and the associated τ_as) and an interpolation parameter (IP) that provides the fraction of each of the aerosol models to be used in the computation of L_{Other}. Using the approximation $t = t^*$ for each aerosol model (with the t^*s computed from the aerosol models and optical thicknesses with look up tables already provided in the Gordon and Wang algorithm) and interpolating between them, the water-leaving radiance and the chlorophyll concentration (Chl) is computed. Then, with Chl, the Morel and Gentili f/Q (providing the appropriate $\langle L_u^{(m)} \rangle$s) is determined through linear interpolation using log(Chl). From this, and the two aerosol models, the two appropriate values of δ_{SS} are found and then interpolation (using IP) is carried out as in the Gordon and Wang algorithm. The resulting value of δ_{SS} is then used to provide an improved L_w. Using the approximate t^* as opposed

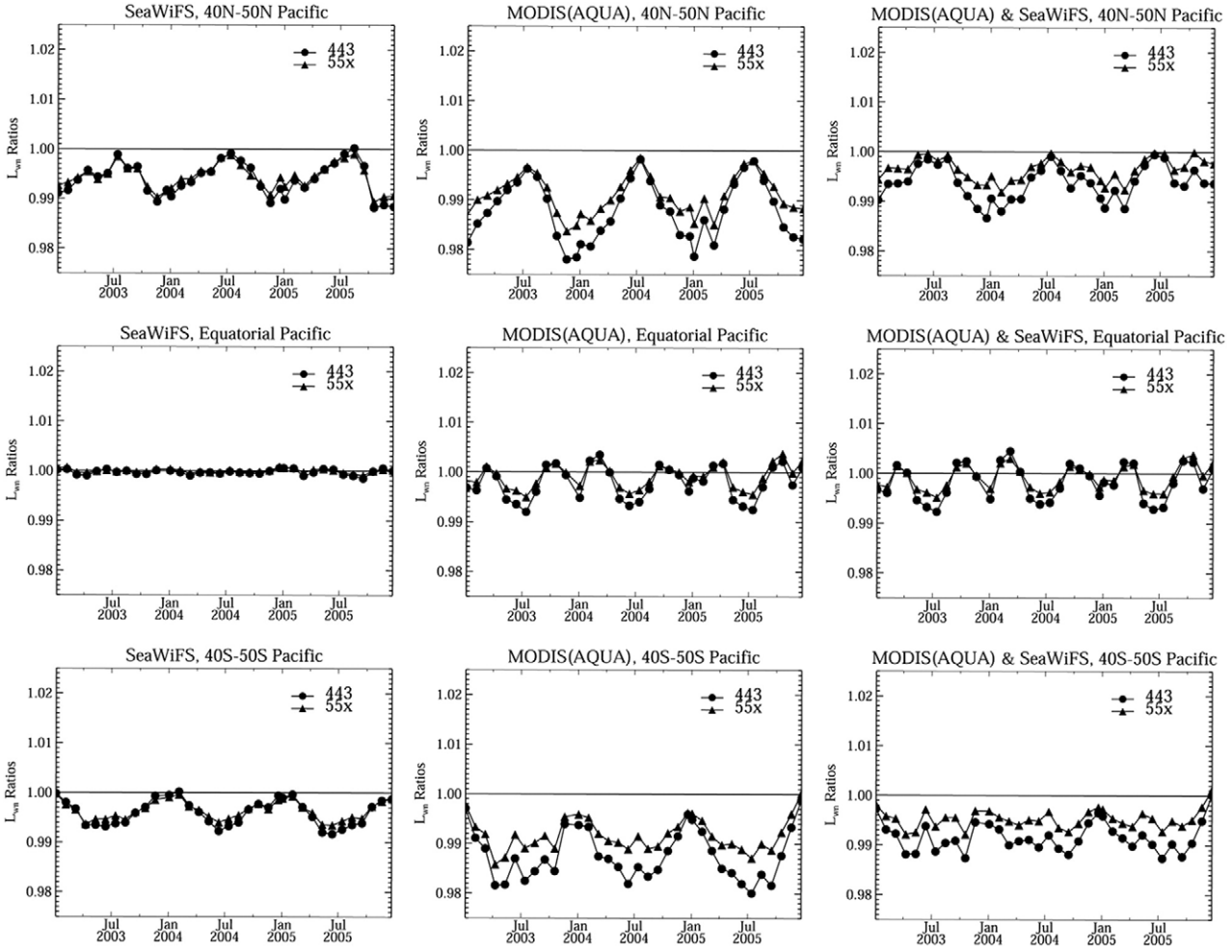

Fig. 7. Four-day zonal means (at 32-day intervals) in the Pacific Ocean showing the result of correcting the diffuse transmittance for bidirectional effects. The top row is the 4-day zonal mean from Latitude 40°N to 50°N, the middle row is the 4-day zonal mean from Latitude 10°S to 10°N, and the bottom row is the 4-day zonal mean from Latitude 40°S to 50°S. The first column provides the ratio of the 4-day zonal mean SeaWiFS-retrieved L_w using the corrected t to that retrieved using t^*, the second the same ratio for MODIS, and the third column is the second column divided by the first column, i.e., the MODIS L_w ratio divided by the SeaWiFS L_w ratio. In the legend, 55x stands for the 555 nm (SeaWiFS) or the 551 nm (MODIS) bands. For each graph the vertical scale runs from 0.975 to 1.025, while the horizontal axis is from Jan. 2003 to Jan 2006.

to the exact t has little influence on the retrieved Chl, so the procedure does not need to be iterated.

This procedure was applied to the computation of δ_{SS} along a SeaWiFS scan line in the vicinity of the Hawaiian Islands. The results at 412 nm are provided in Fig. 6. The retrieved chlorophyll concentration was ~0.1 to 0.2 mg/m^3. The sun angle is 20.6° near the scan center. Pixel number 0 is at the eastern edge of the scan and number 1284 is at the western edge. At the edges of the scan $\theta = 74.16°$. The figure shows that δ_{SS} < approximately 0.01 over most of the scan, but can reach 0.05 to 0.06 near the edges which would correspond to an error of 5 to 6% in the retrieved L_w using t^*. This suggests that if the viewing is restricted to pixels between ~100 and 1150, the t^*-induced error will be less than about 1%. These pixel numbers correspond to θ less than about 60° (the exact pixel numbers for $\theta = 60°$ are 106 and 1164).

Fig. 6 suggests that if the range in viewing angles is restricted to θ less than about 60°, the t^*-induced error in the comparison of data from sensors with different orbital characteristics might be reduced to the 1 to 2% level. This was tested by applying the procedure to SeaWiFS and MODIS (AQUA) data covering the January 2003 through January 2006. Fig. 7 provides the results of this processing for the Pacific Ocean between Longitudes 140°W and 179°W. In the figure, the top row is the 4-day zonal mean (at 32-day intervals) from Latitude 40°N to 50°N, the middle row is the 4-day zonal mean from Latitude 10°S to 10°N, and the bottom row is the 4-day zonal mean from Latitude 40°S to 50°S. The first column provides the ratio of the 4-day zonal mean SeaWiFS-retrieved L_w using the corrected diffuse transmittance to that retrieved using t^*, the second the same ratio for MODIS, and the third column is the second column divided by the first column, i.e., the MODIS L_w ratio divided by the SeaWiFS L_w ratio.

Consider the SeaWiFS ratios (the first column). The most obvious feature of the graphs is their periodic nature with the expected period of one year, and opposite phase in the Northern and Southern hemispheres. The maximum correction to the SeaWiFS-retrieved L_ws is 1% (because of the restricted scan), and the corrections in the blue and green are similar, showing that nearly the same Chl (retrieved using the blue–green ratio) will in fact be derived from the corrected and the uncorrected radiances. Interestingly, there is virtually no correction near the Equator. This is likely due to the sun-glint-avoidance tilting capability of SeaWiFS. MODIS (the second column) shows a similar behavior, but with a larger correction (up to 2%). In the Equatorial belt MODIS has a periodic behavior but with a period of six months and a smaller correction than the higher-latitude belts.

To try to understand the effect of the correction on the merging (or comparison) of SeaWiFS and MODIS data we divided column two by column one and present this in the third column. If the two sets of corrected data were significantly different, i.e., the correction were more important for one sensor than the other (or phased differently), it would clearly show up in this ratio. The third column shows that the maximum t^*-induced error in the merged data is a little over 1% at the higher latitudes and even less at the lower latitudes.

5. Concluding remarks

We have provided a first-order correction to the diffuse transmittance (water surface to space) for bidirectional effects in the water-leaving radiance. The first-order correction is shown to capture much of the variability of $t(\hat{\xi})$ with viewing direction. The correction is then modified in a manner that allows efficient operation in an image processing environment. Application to SeaWiFS and MODIS (AQUA) suggests that the bidirectionally-induced error in the diffuse transmittance could reach 5–6% at large scan angles, but will result in an error ~1% in the comparison of their normalized water-leaving radiances as long as the scans are restricted to $\theta < 60°$. Fig. 8 provides the ratio of the 4-day zonal mean (at 32-day intervals) normalized water-leaving radiances (MODIS/SeaWiFS) for the region corresponding to the top row of Fig. 7. This figure was prepared using the corrected diffuse transmittance; however, using t^* instead induces only minor changes. It shows that the MODIS-to-SeaWiFS variability is considerably above that induced by using t^* in place of t. From these results we conclude that (for the mesotrophic waters considered here with $0.17 \le \text{Chl} \le 0.4$ mg/m^3) normalized water-leaving radiance retrievals from these two sensors at a given location can be merged without regard for the bidirectionally-induced error in the diffuse transmittance if $\theta < 60°$, i.e., although not strictly correct the error in using t^* in place of t is well below the error that could be expected from other sources, e.g., the estimate of L_{Other}. For values of Chl greater than ~1 to 3 mg/m^3, L_w in the blue is considerably reduced, magnifying the importance of error in L_{Other} and therefore rendering error in t even less important. We note that these observations are derived by examining SeaWiFS and MODIS, but are likely to be valid for intercomparison of any other polar-orbiting sensor with equatorial crossing times between 1030 and 1330 h (local). The influence of bidirectional effects in comparing data from other sensors with significantly

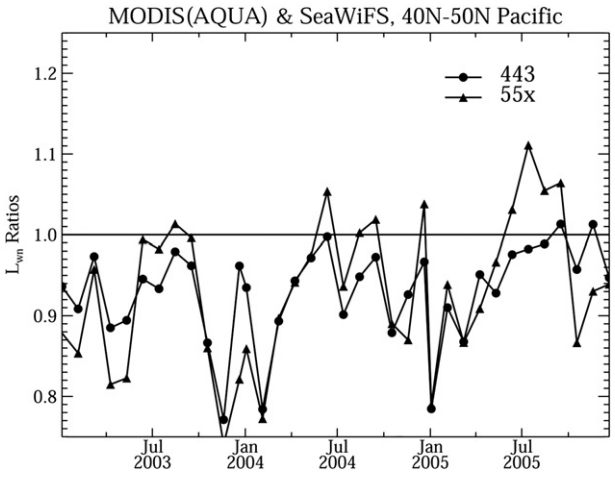

Fig. 8. Four-day zonal mean (at 32-day intervals) of the ratio (MODIS/SeaWiFS) of the normalized water-leaving radiance for Latitude belt 40°N to 50°N in the Pacific Ocean. These data have been corrected for the diffuse transmittance error. The uncorrected comparison is similar to the corrected comparison. Note that the variability is considerably greater than the 1% differences in the ratios shown in Fig. 7.

different orbital characteristics should be examined on an individual basis using the techniques presented here. Finally, investigators interested in utilizing data for $\theta > 60°$ should consider using the correction to t^* developed here.

Acknowledgment

The authors thank K. Voss for providing Fig. 4. This work received support from NASA Contract NNG04HZ21C.

References

Gordon, H. R., Clark, D. K., Brown, J. W., Brown, O. B., Evans, R. H., & Broenkow, W. W. (1983). Phytoplankton pigment concentrations in the Middle Atlantic Bight: Comparison between ship determinations and Coastal Zone Color Scanner estimates. *Applied Optics*, *22*, 20−36.

Gordon, H. R., Clark, D. K., Mueller, J. L., & Hovis, W. A. (1980). Phytoplankton pigments derived from the Nimbus-7 CZCS: Initial comparisons with surface measurements. *Science*, *210*, 63−66.

Gordon, H. R., & Morel, A. Y. (1983). *Remote assessment of ocean color for interpretation of satellite visible imagery: A review.* Springer-Verlag 114 pp.

Gordon, H. R., & Wang, M. (1994). Retrieval of water-leaving radiance and aerosol optical thickness over the oceans with SeaWiFS: A preliminary algorithm. *Applied Optics*, *33*, 443−452.

Hooker, S. B., Esaias, W. E., Feldman, G. C., Gregg, W. W., & McClain, C. R., (1992). SeaWiFS Technical Report Series: Volume 1, An Overview of SeaWiFS and Ocean Color, NASA, Greenbelt, MD, Technical Memorandum 104566, July 1992.

Hovis, W. A., Clark, D. K., Anderson, F., Austin, R. W., Wilson, W. H., Baker, E. T., et al. (1980). Nimbus 7 coastal zone color scanner: System description and initial imagery. *Science*, *210*, 60−63.

Morel, A., Antoine, D., & Gentili, B. (2002). Bidirectional reflectance of oceanic waters: Accounting for Raman emission and varying particle scattering phase function. *Applied Optics*, *41*, 6289−6306.

Morel, A., & Gentili, B. (1991). Diffuse reflectance of oceanic waters: Its dependence on Sun angle as influenced by the molecular scattering contribution. *Applied Optics*, *30*, 4427−4438.

Morel, A., & Gentili, B. (1993). Diffuse reflectance of oceanic waters. II. Bidirectional aspects. *Applied Optics*, *32*, 6864−6879.

Morel, A., & Gentili, B. (1996). Diffuse reflectance of oceanic waters. III. Implication of bidirectionality for the remote sensing problem. *Applied Optics*, *35*, 4850−4862.

Morel, A., Voss, K. J., & Gentili, B. (1995). Bidirectional reflectance of oceanic waters: A comparison of modeled and measured upward radiance fields. *Journal of Geophysical Research*, *100C*, 13,143−13,150.

Salomonson, V. V., Barnes, W. L., Maymon, P. W., Montgomery, H. E., & Ostrow, H. (1989). MODIS: Advanced facility instrument for studies of the Earth as a system. *IEEE Geoscience and Remote Sensing Society Newsletter*, *27*, 145−152.

Shettle, E. P. & Fenn, R. W., (1979). Models for the aerosols of the lower atmosphere and the effects of humidity variations on their optical properties, Air Force Geophysics Laboratory, Hanscomb AFB, MA 01731, AFGL-TR-79-0214.

Yang, H., & Gordon, H. R. (1997). Remote sensing of ocean color: Assessment of the water-leaving radiance bidirectional effects on the atmospheric diffuse transmittance. *Applied Optics*, *36*, 7887−7897.